MARTIN MARIETTA ENERGY SYSTEMS LIBRARIES

3 4456 0316246 8

ORNL/TM-11561

ornl

OAK RIDGE NATIONAL LABORATORY

MARTIN MARIETTA

QUICKGUN: An Algorithm for Estimating the Performance of Two-Stage Light Gas Guns

S. L. Milora
S. K. Combs
M. J. Gouge
R. W. Kincaid

OAK RIDGE NATIONAL LABORATORY
CENTRAL RESEARCH LIBRARY
CIRCULATION SECTION
4500N ROOM 175
LIBRARY LOAN COPY
DO NOT TRANSFER TO ANOTHER PERSON
If you wish someone else to see this report, send in name with report and the library will arrange a loan.

OPERATED BY
MARTIN MARIETTA ENERGY SYSTEMS, INC.
FOR THE UNITED STATES
DEPARTMENT OF ENERGY

This report has been reproduced directly from the best available copy.

Available to DOE and DOE contractors from the Office of Scientific and Technical Information, P.O. Box 62, Oak Ridge, TN 37831; prices available from (615) 576-8401, FTS 626-8401.

Available to the public from the National Technical Information Service, U.S. Department of Commerce, 5285 Port Royal Rd., Springfield, VA 22161.
NTIS price codes—Printed Copy: A03 Microfiche A01

This report was prepared as an account of work sponsored by an agency of the United States Government. Neither the United States Government nor any agency thereof, nor any of their employees, makes any warranty, express or implied, or assumes any legal liability or responsibility for the accuracy, completeness, or usefulness of any information, apparatus, product, or process disclosed, or represents that its use would not infringe privately owned rights. Reference herein to any specific commercial product, process, or service by trade name, trademark, manufacturer, or otherwise, does not necessarily constitute or imply its endorsement, recommendation, or favoring by the United States Government or any agency thereof. The views and opinions of authors expressed herein do not necessarily state or reflect those of the United States Government or any agency thereof.

ORNL/TM-11561
Dist. Category UC-420

Fusion Energy Division

QUICKGUN: AN ALGORITHM FOR ESTIMATING THE PERFORMANCE OF TWO-STAGE LIGHT GAS GUNS

S. L. Milora
S. K. Combs
M. J. Gouge
R. W. Kincaid
North Carolina State University

Date Published: September 1990

Prepared for the
Office of Fusion Energy
Budget Activity No. AT 15 01 02 7

Prepared by the
OAK RIDGE NATIONAL LABORATORY
Oak Ridge, Tennessee 37831-6285
operated by
MARTIN MARIETTA ENERGY SYSTEMS, INC.
for the
U.S. DEPARTMENT OF ENERGY
under contract DE-AC05-84OR21400

MARTIN MARIETTA ENERGY SYSTEMS LIBRARIES

3 4456 0316246 8

CONTENTS

ABSTRACT v
1. INTRODUCTION 1
2. COMPONENT DESCRIPTIONS 3
   2.1 RESERVOIR 3
   2.2 VALVE 4
   2.3 FIRST STAGE 4
   2.4 SECOND STAGE 5
   2.5 LAUNCH TUBE 7
3. RESULTS 11
4. CONCLUSIONS 14
ACKNOWLEDGMENT 15
REFERENCES 17

ABSTRACT

An approximate method is described for solving the equation of motion of a projectile accelerated by a two-stage light gas gun that uses high-pressure (<100-bar) gas from a storage reservoir to drive a piston to moderate speed (<400 m/s) for the purpose of compressing the low molecular weight propellant gas (hydrogen or helium) to high pressure (1000 to 10,000 bar) and temperature (1000 to 10,000 K). Zero-dimensional, adiabatic (isentropic) processes are used to describe the time dependence of the ideal gas thermodynamic properties of the storage reservoir and the first and second stages of the system. A one-dimensional model based on an approximate method of characteristics, or wave diagram analysis, for flow with friction (nonisentropic) is used to describe the nonsteady compressible flow processes in the launch tube. Linear approximations are used for the characteristic and fluid particle trajectories by averaging the values of the flow parameters at the breech and at the base of the projectile. An assumed functional form for the Mach number at the breech provides the necessary boundary condition. Results of the calculation are compared with data obtained from two-stage light gas gun experiments at Oak Ridge National Laboratory for solid deuterium and nylon projectiles with masses ranging from 10 to 35 mg and for projectile speeds between 1.6 and 4.5 km/s. The predicted and measured velocities generally agree to within 15%.

1. INTRODUCTION

Single-stage light gas guns operating with helium and hydrogen propellant have been used as drivers for advanced plasma fuel injection systems for several years.[1–8] These devices can launch solid hydrogen, deuterium, and tritium[8] pellets with diameters of 1 to 6 mm at speeds of less than 2 km/s. The two-stage light gas gun approach has been adopted as a way to improve the performance of pellet injection systems in anticipation of more demanding applications on reactor-like devices, where speeds above ≈5 km/s will be required for deep penetration in the hot plasma. Present developmental systems operate at speeds of about 3 km/s with deuterium pellets and at speeds above 4 km/s when the deuterium ice is protected from hot gas erosion by a sabot.[9–14]

We present an approximate model to determine the dynamics and performance of two-stage light gas gun systems of the type shown in Fig. 1. A valve separates the high-pressure gas storage reservoir from the first stage, which is defined as the region of the pump tube between the valve outlet and the rear face of the piston. The thermodynamic parameters of the reservoir and first stage are calculated from zero-dimensional (0-D) expressions for mass and energy conservation assuming adiabatic conditions and ideal gas relationships. The valve that controls the flow of gas between these two stations is modeled as an equivalent sharp-edge orifice. The second stage incorporates the region between the front face of the piston and the entrance to the launch tube (breech). This is also treated in a 0-D approximation with applicable expressions for mass and energy conservation. Acceleration of the piston is determined by the pressure imbalance between the first and second stages. Because friction and heat transfer are neglected, all processes up to the breech location are isentropic. By operating with low initial pressure (usually subatmospheric) in the second stage, very large compression ratios are developed, and high pressures and temperatures are realized at the breech as the kinetic energy of the piston is converted ideally into work on the second-stage gas. The nonsteady equations of motion in the launch tube are described by a one-dimensional (1-D) model and are solved algebraically by an approximate method of characteristics with an assumed functional form for the breech Mach number. The latter step effectively relates the pressure at the projectile base to the conditions at the breech. Ideal gas relationships are assumed for the thermodynamic properties of the propellant gas, and the effect of friction is modeled as a retarding force (with dissipation) acting on the fluid element at the inner wall of the launch tube.

ORNL-DWG 90M-2782 FED

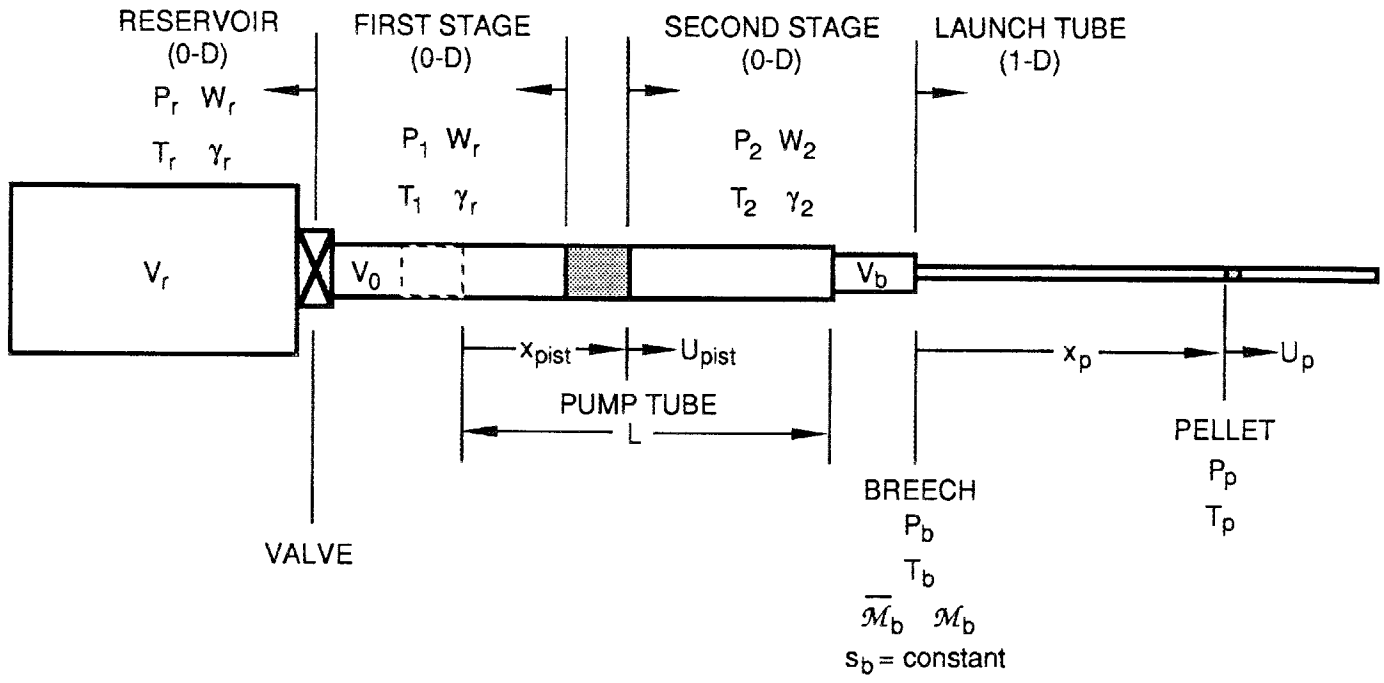

Fig. 1. Schematic of two-stage light gas gun. Symbols are defined in the text.

This treatment is similar to an earlier model presented by Riva and Reggiori,[15] who considered only isentropic flow in the launch tube but incorporated additional effects such as heat transfer to the second-stage walls and mass transfer between the first and second stages, which results from an imperfect seal at the piston–pump tube interface. In our treatment, we employ a less rigorous, or approximate, method of characteristics for the solution in the launch tube. As mentioned, friction is taken into account, and a model is used to describe the flow through the valve separating the reservoir from the first stage.

In Sect. 2, we present the mathematical descriptions of the various components of the system shown in Fig. 1. In Sect. 3, example solutions are presented, and the results are compared with data obtained from the ORNL two-stage gas gun facility. Conclusions are given in Sect. 4.

2. COMPONENT DESCRIPTIONS

2.1 RESERVOIR

The conditions in the reservoir are computed using 0-D models expressing conservation of energy and mass within the reservoir volume V_r:

$$\frac{d(m_r e_r)}{dt} = -\dot{m}_r h_r \quad , \tag{1}$$

$$\frac{dm_r}{dt} = -\dot{m}_r \quad , \tag{2}$$

where e_r and h_r are the specific internal energy and enthalpy of the gas, $m_r = \rho_r V_r$ is the mass in the reservoir, and $\dot{m}_r$ represents the mass efflux rate through the valve separating the reservoir from the first stage. The mass density ρ_r is related to the pressure P_r and temperature T_r by the ideal gas equation of state,

$$P_r = \rho_r R_r T_r \quad . \tag{3}$$

Similarly, the internal energy and enthalpy are related to the temperature by ideal gas specific heats and the specific heat ratio γ_r,

$$e_r = C_{v_r} T_r \quad , \tag{4a}$$

$$h_r = C_{p_r} T_r \quad , \tag{4b}$$

where $C_{v_r} = R_r/(\gamma_r - 1)$, $C_{p_r} = R_r[\gamma_r/(\gamma_r - 1)]$, and $R_r = \mathcal{R}/W_r$; the universal gas constant and molecular weight of the gas are denoted by $\mathcal{R}$ and W_r, respectively.

2.2 VALVE

The valve separating the reservoir from the first stage is modeled as a sharp-edge orifice with an equivalent diameter D_{eq} and a response time to fully open t_{resp}. A simple linear ramp function is used to approximate the opening characteristics of the valve. For compressible flow, the mass flow rate through the valve is dependent on the valve area A_v, the reservoir temperature and pressure, and the downstream pressure P_1; however, for values of the pressure ratio below a certain critical value, the flow will be choked, and consequently the throughput will depend only on the upstream conditions. The mass flow rate is therefore written in the following form,[16] which is valid for any back pressure:

$$\dot{m}_r = C_d A_v g_2 \frac{P_r}{\sqrt{T_r}} \times \begin{cases} 1 \ , & P_1 < P_{\text{crit}} \\ \dfrac{g_1}{g_2}\left(\dfrac{P_1}{P_r}\right)^{1/\gamma_r}\left[1-\left(\dfrac{P_1}{P_r}\right)^{(\gamma_r-1)/\gamma_r}\right]^{1/2} \ , & P_1 \geq P_{\text{crit}} \end{cases} \ , \quad (5)$$

where

$$P_{\text{crit}} = P_r \left(\frac{2}{\gamma_r+1}\right)^{\gamma_r/(\gamma_r-1)}$$

and

$$A_v = \frac{\pi}{4} D_{\text{eq}}^2 \times \begin{cases} \dfrac{t}{t_{\text{resp}}} \ , & t \leq t_{\text{resp}} \\ 1 \ , & t > t_{\text{resp}} \end{cases} \ .$$

In Eq. (5), C_d is the valve discharge coefficient ($\approx$0.8) and the constants g_1 and g_2 are given by

$$g_1 = \left[\frac{2\gamma_r}{R_r(\gamma_r-1)}\right]^{1/2} \ , \quad g_2 = \left[\frac{\gamma_r}{R_r}\left(\frac{2}{\gamma_r+1}\right)^{(\gamma_r+1)/(\gamma_r-1)}\right]^{1/2} \ .$$

2.3 FIRST STAGE

As in the reservoir, the conditions in the first stage, which comprises the volume between the valve and the rear face of the piston, are computed from the applicable 0-D expressions for energy and mass conservation:

$$\frac{d(m_1 e_1)}{dt} = \dot{m}_r h_r - P_1 U_{\text{pist}} A_{\text{pist}} \ , \quad (6)$$

$$\frac{dm_1}{dt} = \dot{m}_r \quad , \tag{7}$$

where the subscript 1 denotes the first stage and $U_{\text{pist}} = dx_{\text{pist}}/dt$ and A_{pist} represent the speed and cross-sectional area of the piston, respectively. In Eq. (6), the first term on the right-hand side represents the enthalpy convected into the first stage by the gas exiting the reservoir, and the second term represents the expansion work done by the first-stage gas against the moving piston. The mass density in the first stage is related to the total mass contained within its volume, which consists of an initial fixed volume V_0 and the volume swept out by the piston as it moves,

$$m_1 = \rho_1(V_0 + x_{\text{pist}}A_{\text{pist}}) \quad , \tag{8}$$

where x_{pist} is the position of the the piston relative to its initial resting position.

When friction between the piston and the pump tube bore is neglected, the motion of the piston is completely specified by the pressure imbalance between the first and second stages:

$$\frac{d^2x_{\text{pist}}}{dt^2} = \frac{dU_{\text{pist}}}{dt} = \frac{(P_1 - P_2)A_{\text{pist}}}{M_{\text{pist}}} \quad , \tag{9}$$

where M_{pist} is the piston mass and P_2 is the pressure in the second stage.

The description of the first stage is completed by the ideal gas relationships for pressure, internal energy, and enthalpy, which, when the first-stage and reservoir working gases are the same, are

$$P_1 = \rho_1 R_r T_1 \ , \quad e_1 = C_{v_r} T_1 \ , \quad h_1 = C_{p_r} T_1 \quad .$$

2.4 SECOND STAGE

The second stage is defined as the region between the front face of the piston and the breech of the gun (entrance to the launch tube and initial position of the projectile). This region is also modeled as a 0-D entity whose volume changes as the piston traverses the pump tube. In addition, a fixed volume V_b is included in the calculation to account for the volume of components located between the end, or head, of the pump tube and the breech. Mass loss from the second stage is estimated by assuming that gas escaping into the launch tube as a result of the projectile movement does so at a constant, or average, breech Mach number $\overline{\mathcal{M}}_b$. The mass loss is included only after the projectile has started to move. In

the code, this condition is satisfied when the second-stage pressure exceeds the specified projectile release pressure, $P_{\rm rel}$. The relevant expressions for energy and mass conservation are

$$\frac{d(m_2 e_2)}{dt} = \begin{cases} P_2 U_{\rm pist} A_{\rm pist} \ , & P_2 < P_{\rm rel} \\ P_2 U_{\rm pist} A_{\rm pist} - \dot{m}_b \left(h_2 + \frac{1}{2} U_b^2 \right) \ , & P_2 \geq P_{\rm rel} \end{cases} \tag{10}$$

and

$$\frac{dm_2}{dt} = \begin{cases} 0 \ , & P_2 < P_{\rm rel} \\ -\dot{m}_b \ , & P_2 \geq P_{\rm rel} \end{cases} \ , \tag{11}$$

respectively, where the subscript 2 denotes the second stage and the subscript b denotes the breech. The first term on the right-hand side of Eq. (10) represents the work done on the second-stage gas by the advancing piston, and the second term represents the energy loss associated with the mass flow rate at the breech, $\dot{m}_b = \rho_b U_b A_b$. In the energy balance we include also the kinetic energy of the gas escaping at speed $U_b = \overline{\mathcal{M}}_b a_b$, where $a_b = \sqrt{\gamma_2 R_2 T_b}$ is the sound speed evaluated at the breech. The mass contained at any time within the second stage is related to the volume and mass density by the expression

$$m_2 = \rho_2 V_b + \rho_2 A_{\rm pist}(L - x_{\rm pist}) \ ,$$

where L is the active length of the pump tube. The remaining thermodynamic conditions in the second stage are given by the relevant ideal gas relationships:

$$P_2 = \rho_2 R_2 T_2 \ , \ R_2 = \frac{\mathcal{R}}{W_2} \ , \ e_2 = C_{v_2} T_2 \ , \ C_{v_2} = \frac{R_2}{\gamma_2 - 1} \ ,$$
$$h_2 = C_{p_2} T_2 \ , \ C_{p_2} = R_2 \frac{\gamma_2}{\gamma_2 - 1} \ ,$$

where the previous definitions apply. Finally, the thermodynamic properties at the breech are related to their corresponding values in the second stage by well-known gasdynamic expressions[17] applicable to steady flow in nozzles:

$$P_b = P_2 \psi^{[\gamma_2/(\gamma_2-1)]} \ , \ \rho_b = \rho_2 \psi^{[1/(\gamma_2-1)]} \ , \ \psi = \left(1 + \frac{\gamma_2 - 1}{2} \overline{\mathcal{M}}_b{}^2 \right)^{-1} \ .$$

With the assumption of a fixed Mach number at the breech, the parameters of the system are completely determined up to and including the breech location and are thus independent of the dynamics occurring in the launch tube. This simplification effectively decouples the solutions for the reservoir, first stage, and

second stage from the solution for the projectile motion while providing one boundary condition needed to obtain an approximate solution for the projectile motion in the launch tube. In the code, the parameters of the reservoir and the first and second stages are computed first by solving this system of coupled differential equations numerically. The projectile motion is computed from the conditions determined at the breech, as described in Sect. 2.5.

2.5 LAUNCH TUBE

An approximate 1-D model based on the method of characteristics[18] is used to solve numerically for the nonsteady compressible flow in the launch tube and the resultant projectile motion. In contrast to the treatment of the reservoir and the first and second stages, a 1-D model is required to relate the pressure at the base of the projectile, which provides the acceleration force, to the breech pressure. In the first and second stages, the piston speed is usually much smaller than the sound speed, and consequently the assumption that the pressure equilibrates instantaneously throughout the respective volumes (i.e., that it is 0-D) is usually justified for computing the piston motion. However, in the launch tube and, in particular, at high projectile speeds and at distances far from the breech, rarefaction waves propagating rearward from the base of the projectile tend to negate the forward-propagating compression waves originating at the breech, and this can lead to significant reductions in the pressure at the projectile base relative to the instantaneous value at the breech.

The method of solution employed is based on the approach suggested by Siegel,[19] whereby the approximate projectile base pressure is determined as a function of time for isentropic flow by specifying a fixed Mach number at the breech and by taking average values for the sound speed and gas speed along a characteristic curve. We have refined this method by incorporating the effects of friction (nonisentropic flow) and by including a more flexible functional form for the breech Mach number that better approximates the conditions at the breech. This technique is illustrated graphically in Fig. 2, a wave diagram in the x–t plane describing the projectile trajectory and the trajectories of a fluid particle and a characteristic curve. Both have been linearized by taking as their respective velocities simple averages of the values pertaining at the breech and projectile positions. The curve labeled "$\mathcal{P}$ characteristic" is the trajectory of a forward-propagating pressure disturbance traveling at the local sound speed, a, in the reference frame of the gas moving at

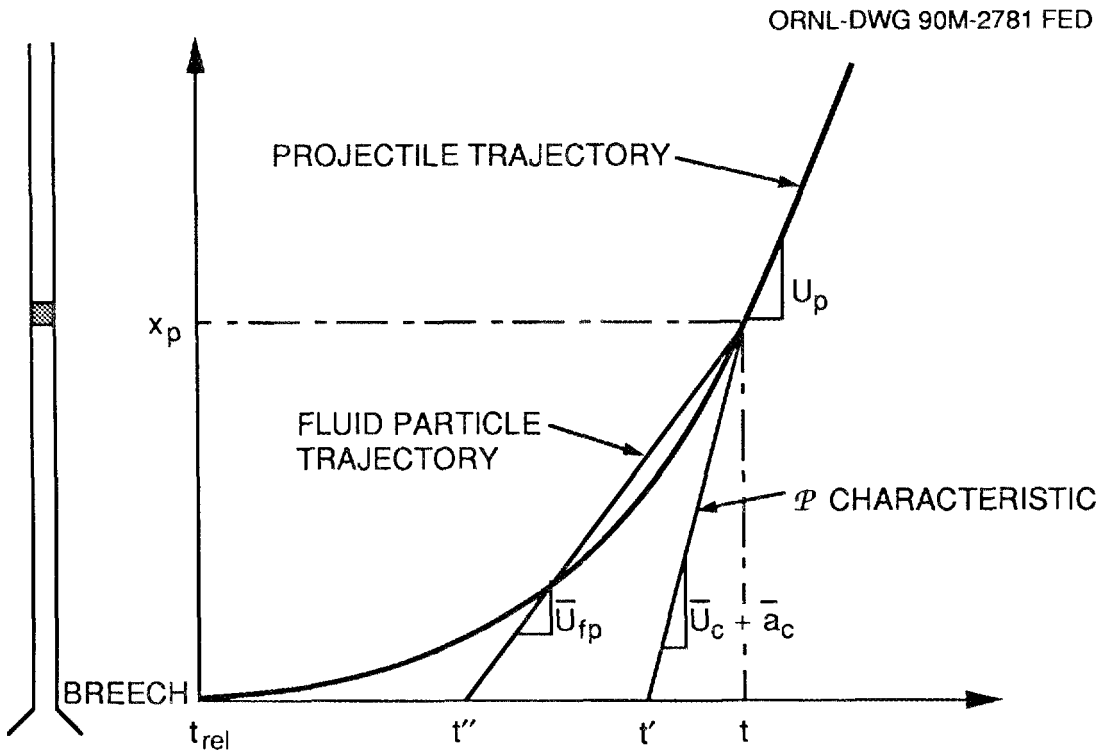

Fig. 2. Wave diagram for fluid and projectile motion in launch tube.

speed U. In the linear approximation, it intercepts the projectile at time t after having left the breech at an earlier time t', defined by

$$\frac{x_p}{t - t'} = \overline{U}_c + \bar{a}_c \quad , \tag{12}$$

where $\overline{U}_c = [U_b(t') + U_p(t)]/2$ and $\bar{a}_c = [a_b(t') + a_p(t)]/2$ represent respectively the fluid speed and sound speed averages on the characteristic. Following Siegel,[19] we specify a value for the breech Mach number, $\mathcal{M}_b$, which determines the value of $U_b(t')$. A functional form is assumed that approaches zero in the limit of low projectile velocity and increases asymptotically to $\overline{\mathcal{M}}_b$ as the projectile accelerates to speeds in excess of the fluid velocity at the breech,

$$\mathcal{M}_b = \overline{\mathcal{M}}_b U_p(t)/[\overline{\mathcal{M}}_b a_b(t') + U_p(t)] \approx \begin{cases} \dfrac{U_p(t)}{a_b(t')} \ , & U_p \ll \overline{\mathcal{M}}_b a_b \\ \overline{\mathcal{M}}_b \ , & U_p \gg \overline{\mathcal{M}}_b a_b \end{cases} \quad . \tag{13}$$

It follows that the fluid velocity at the breech is given by $U_b(t') = \mathcal{M}_b a_b(t')$.

To complete the solution, an additional relationship is required for the sound speed at the projectile base. The necessary information is obtained from consideration of the manner in which the Riemann variable $\mathcal{P}$ varies on a characteristic, where $\mathcal{P} = [2/(\gamma_2 - 1)]a + U$ and $\Delta\mathcal{P} = \mathcal{P}_p(t) - \mathcal{P}_b(t')$.

For flow with friction in a constant-area duct, the change in $\mathcal{P}$ between two locations on a characteristic is dependent on the entropy of the two states and the resultant body force exerted on the gas by the wall shear stress. The entropy increase in the launch tube is a result of heat dissipation in the gas resulting from the friction force exerted at the wall. By once again taking average values, we obtain an estimate of the change in $\mathcal{P}$ between t and t' (ref. 18),

$$\Delta\mathcal{P} = \frac{\overline{U}_c[s_p(t) - s_b(t')]}{R_2} - \frac{\lambda(t-t')\overline{U}_c^2}{2D_b}\left[1 + (\gamma_2 - 1)(\overline{U}_c/\bar{a}_c)\right] \quad , \tag{14}$$

where s is the specific fluid entropy and λ is the friction coefficient, defined in terms of the pressure gradient within the launch tube as

$$\nabla P = -\lambda\frac{\rho U^2}{2D_b} \quad .$$

For fully developed pipe flow, the friction coefficient varies only weakly with the Reynolds number; consequently, in the calculation we assume $\lambda \approx \text{const} = 0.02$ (ref. 16).

The fluid entropy change between the breech and projectile is calculated from the heat dissipated in the gas by the wall friction force acting on a fluid particle moving between the two locations. Referring to Fig. 2, a fluid particle leaving the breech at time t'' at average speed $\overline{U}_{fp}$ will intercept the projectile at time t according to

$$\overline{U}_{fp} = \frac{U_b(t'') + U_p(t)}{2} = \frac{x_p}{t - t''} \tag{15}$$

As before, we relate the fluid velocity at the breech to an assumed Mach number by $U_b(t'') = \mathcal{M}_b a_b(t'')$, where

$$\mathcal{M}_b = \overline{\mathcal{M}}_b U_p(t)/[\overline{\mathcal{M}}_b a_b(t'') + U_p(t)] \quad .$$

The rate of entropy production moving with a fluid particle is given in terms of previously defined parameters and the average sound speed by[18]

$$\dot{s} = \frac{\lambda\gamma_2 R_2|\overline{U}_{fp}|^3}{2D_b\bar{a}_{fp}^2} \quad , \tag{16}$$

where

$$\bar{a}_{fp} = \frac{a_b(t'') + a_p(t)}{2} \quad .$$

In our approximate linear treatment, it follows that the specific entropy at the projectile position is given by

$$s_p(t) = s_b(t'') + (t - t'')\dot{s} \quad . \tag{17}$$

Because of the assumption that the flow for all stages up to and inclusive of the breech is isentropic, $s_b(t) = \text{const}$, and consequently Eq. (14) reduces to

$$\Delta\mathcal{P} = \frac{\overline{U}_c\dot{s}(t - t'')}{R_2} - \frac{\lambda(t - t')\overline{U}_c^2}{2D_b}\left[1 + (\gamma_2 - 1)(\overline{U}_c/\bar{a}_c)\right] \quad . \tag{18}$$

From the definitions of the Riemann variable and $\Delta\mathcal{P}$, the sound speed at the projectile is

$$a_p(t) = a_b(t') + \frac{\gamma_2 - 1}{2}\left[\Delta\mathcal{P} + U_b(t') - U_p(t)\right] \quad . \tag{19}$$

The projectile base pressure, which provides the acceleration force, is given by the alternate form of the equation of state,

$$P_p(t) = P_b(t')\left[\frac{a_p(t)}{a_b(t')}\right]^{2\gamma_2/(\gamma_2-1)} \exp\{-[s_p(t) - s_b(t')]/R_2\} \quad . \tag{20}$$

With $s_b(t) = \text{const}$, Eq. (20) reduces to

$$P_p(t) = P_b(t')\left[\frac{a_p(t)}{a_b(t')}\right]^{2\gamma_2/(\gamma_2-1)} \exp\{-[\dot{s}(t - t'')]/R_2\} \quad . \tag{21}$$

Finally, the projectile's speed (which is equal to the gas velocity at the projectile location) and position are determined in terms of the base pressure and the mass and cross-sectional area of the projectile by the equation of motion,

$$\frac{d^2x_p}{dt^2} = \frac{dU_p}{dt} = \frac{P_pA_p}{M_p} \quad . \tag{22}$$

The computer code QUICKGUN was written to solve this system of equations numerically. At any given time t, with known values of x_p and U_p and the breech conditions as determined previously, Eqs. (12), (15), (18), and (19) are solved iteratively to determine t', t'', $\dot{s}$, and $a_p(t)$. The base pressure is calculated from Eq. (21), and this value is used in Eq. (22) to advance the projectile speed and position to the next time step. The calculation is started at initial time t_{rel} when

the pressure in the second stage P_2 reaches the specified projectile release pressure P_{rel}. The initial conditions are $x_p = U_p = 0$ and $P_p = P_{\text{rel}}$.

3. RESULTS

Results of a QUICKGUN calculation for the conditions given in Table 1 are shown in Fig. 3. The conditions chosen for the calculation correspond to those used

Table 1. Parameters for shot 1210

Input parameters	
Reservoir	
Volume, L	2.2
Gas	Helium
Initial pressure, psi	750
Valve ESEOD, cm	2.22
Valve response time, ms	0.10
Piston mass, g	19.6
Pump tube	
Length, m	1.00
Diameter, cm	2.54
Volume, L	0.506
Gas	Helium
Initial pressure, psi	11.6
Breech volume, cm^3	1
Projectile	
Length, mm	2.80
Diameter, mm	3.90
Density, g/cm^3	1.060
Mass, g	35.437
Release pressure, psi	1000
Output parameters	
Pellet release time, ms	4.110
Piston transit time, ms	4.306
Piston impact speed, m/s	0
Distance of closest approach, cm	0.203

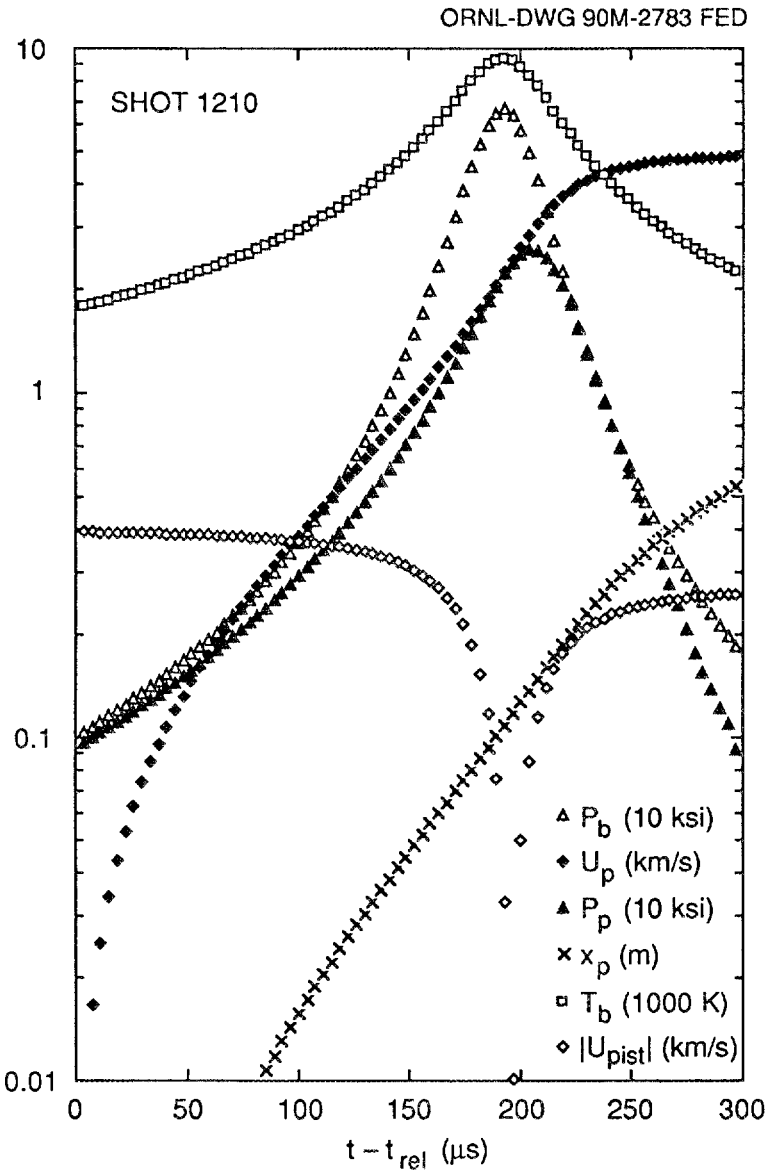

Fig. 3. Results of numerical simulation of shot 1210 for times after projectile release.

in a small two-stage light gas gun facility at ORNL (which has a 2.54-cm-diam, 100-cm-long pump tube) to accelerate 35-mg plastic projectiles to 4.5 km/s (ref. 10). In the experimental case (shot 1210), a 2.22-cm-diam burst disk separated the reservoir from the first stage. This is simulated in the code by setting the valve response time to an arbitrarily small number (0.1 ms) and by taking the burst disk diameter as the valve equivalent sharp-edge orifice diameter (ESEOD). In Fig. 3, the system parameters are shown for times greater than the projectile release time,

t_{rel}, which corresponds to the instant at which the breech pressure reaches the assumed release value of 1000 psi. The calculation was performed for $\overline{\mathcal{M}}_b = 0.3$. The output from the code can be compared to a number of experimentally observed parameters, including muzzle velocity, breech pressure, and the piston transit time, which is defined as the time required for the piston to travel to the point where it reverses direction (distance of closest approach to the end of the pump tube). In this example, the reversal point is calculated to be 0.203 cm from the pump tube end, and this is achieved in a total elapsed time of 4.306 ms, in comparison to an experimental value of 4.4 ms. Although the piston speed was not measured, the code predicts a maximum speed of 400 m/s. As shown in Fig. 3, the calculated maximum breech pressure $P_b = 66,000$ psi, compared to a measured value of 53,900 psi. The shapes of the experimental and calculated breech pressure pulses are similar with full widths at half-maximum of 50 μs and 41 μs, respectively. The calculated projectile base pressure pulse is of comparable width, but it peaks later than the breech pressure. This is a consequence of the finite sound speed of the propellant gas and the distance required for the pressure pulse to propagate from the breech to the projectile location. In the calculation, the projectile speed U_p approaches 4.9 km/s asymptotically, but most of the acceleration is achieved within the first 50 cm of travel. In the experimental case, a speed of 4.5 km/s was measured at the exit of the 1-m-long launch tube.

Some tests were performed using the same gun geometry, but with deuterium pellets and a fast valve to separate the reservoir from the first stage. Code predictions for these cases are compared with the test results in Table 2. The ESEOD for the fast valve, which was developed at ORNL, has not been measured. To estimate its value we have taken the internal diameter of the smallest orifice. The response time of the valve is in the range of 1 to 2 ms; we have assumed 2 ms for the calculation. For the most part, the agreement with the experimental values is good, with a maximum discrepancy in the projectile speed of 13%. Moreover, it can be seen that the pellet velocity discrepancy correlates with the discrepancy in the average piston speed, which is defined as the distance between a pressure transducer used as a time marker, located 8 cm in front of the piston starting position, and the end of the pump tube (the second time marker) divided by the measured time interval for the piston to move between these two locations. The error is reduced considerably when the calculated average piston speed is adjusted to match the measured value (by adjusting the reservoir pressure), as shown in the last row of the table.

Table 2. Simulation results and experimental data from ORNL two-stage light gas gun

	Shot number				
	1210	5041	5064	5088	5089
System parameters					
Projectile material	Nylon	Deuterium	Deuterium	Deuterium	Deuterium
Projectile mass, mg	35	12	12	12	12
Release pressure, psi	1000	300	300	300	300
Piston mass, g	19.6	25.5	25.5	25.5	25.5
Reservoir pressure, psi	750	480	850	1000	1070
Pump tube pressure, psi	11.6	11.6	11.6	11.6	11.6
Valve ESEOD, cm	2.22	0.66	0.66	0.66	0.66
Valve response time, ms	0.1	2	2	2	2
Results					
Average piston speed, m/s					
Measured	289	112	180	187	180
Simulation	296	130	164	175	177
Pellet velocity, km/s					
Measured	4.5	1.6	2.6	2.7	2.8
Simulation	4.92	1.81	2.26	2.45	2.49
Adjusted[a]	4.92	1.60	2.61	2.70	2.57

[a]By adjusting the reservoir pressure.

4. CONCLUSIONS

A simple numerical model has been developed to predict the dynamic performance of small two-stage light gas guns of the type used for high-speed plasma fuel injection systems. The model uses standard 0-D descriptions of the thermodynamic processes (ideal) in the gas storage reservoir and in the first and second stages up to the gun breech location. A model is included to describe the action of the valve separating the reservoir and the first stage. A simplified algebraic algorithm based on the method of characteristics for duct flow with friction is

used to describe the nonsteady flow processes in the launch tube. The model has been benchmarked on a limited number of experiments performed at ORNL with a small two-stage light gas gun facility used to accelerate 4-mm deuterium and nylon pellets to speeds ranging from 1.6 to 4.5 km/s. The model has not been tested at higher speeds (and pressures), where heat transfer and real gas effects may become important and the assumption of 0-D gasdynamic processes in the first and second stages may break down. The effect of friction acting at the interface between the projectile and the launch tube has also been neglected, but, if needed, it can easily be taken into account by modifying the projectile equation of motion with a suitable friction model (velocity power law dependence or increased effective projectile mass). Comparison with more detailed experimental data will be required eventually to determine the limitations of the model.

ACKNOWLEDGMENT

The research of R. W. Kincaid was performed under appointment to the Magnetic Fusion Energy Technology Fellowship program administered by Oak Ridge Associated Universities for the U.S. Department of Energy.

REFERENCES

1. S. L. Milora, "Review of Pellet Fueling of Tokamaks," *J. Vac. Sci. Technol. A* **5**, 2210 (1987).

2. S. K. Combs et al., "Repeating Pneumatic Hydrogen Pellet Injector for Plasma Fueling," *Rev. Sci. Instrum.* **56**, 1173 (1985).

3. S. K. Combs, S. L. Milora, and C. R. Foust, "Simple Pipe Gun for Hydrogen Pellet Injection," *Rev. Sci. Instrum.* **57**, 2636 (1986).

4. S. K. Combs et al., "A Three Barrel Repeating Pneumatic Pellet Injector for Plasma Fueling of the Joint European Torus," *J. Vac. Sci. Technol. A* **6**, 1901 (1988).

5. D. D. Schuresko et al., "Performance Characterization of Pneumatic Single Pellet Injection System," *J. Vac. Sci. Technol. A* **1**, 959 (1983).

6. J. Lafferanderie et al., p. 1367 in *Fusion Technology 1986: Proceedings of the 14th Symposium, Avignon, 1986*, Vol. 2, Pergamon Press, Oxford, 1986.

7. H. Sorensen et al., *Rev. Sci. Instrum.* **58**, 2336 (1987).

8. P. W. Fisher et al., "Tritium Pellet Injector Results," *J. Vac. Sci. Technol. A* **7**, 938 (1989).

9. S. K. Combs et al., "Development of a Two-Stage Light Gas Gun to Accelerate Hydrogen Pellets to High Speeds for Plasma Fueling Applications," *J. Vac. Sci. Technol. A* **7**, 963 (1989).

10. S. K. Combs, C. R. Foust, M. J. Gouge, and S. L. Milora, "Acceleration of Small, Light Projectiles (Including Hydrogen Isotopes) to High Speeds Using a Two Stage Light-Gas Gun," *J. Vac. Sci. Technol. A* **8**, 1814 (1990).

11. A. Reggiori et al., *J. Vac. Sci. Technol. A* **6**, 2556 (1988).

12. A. Reggiori et al., "High Speed Pellet Injection with a Two-Stage Pneumatic Gun," *J. Vac. Sci. Technol. A* **7**, 959 (1989).

13. K. Sonnenberg et al., "Prototype of a High Speed Pellet Launcher for JET," p. 715 in *Fusion Technology 1988: Proceedings of the 15th Symposium, Utrecht, September 1988*, Vol. 1, North-Holland, Amsterdam, 1989.

14. P. Kupschus et al., "Upgrading the JET Pellet Injector with a Two-Stage Light Gas Gun Prototype and Future Planning," p. 1293 in *Proceedings of the 13th Symposium on Fusion Engineering*, Vol. 2, IEEE, New York, 1990.

15. G. Riva and A. Reggiori, "Modelling of Pellet Acceleration by Two-Stage Guns," *Fusion Technol.* **15**, 143 (1989).

16. V. L. Streeter, ed., *Handbook of Fluid Dynamics*, McGraw-Hill, New York, 1961.

17. H. W. Liepmann and A. Roshko, *Elements of Gasdynamics*, Wiley, New York, 1957.

18. G. Rudinger, *Nonsteady Duct Flow*, Dover Publications, Inc., New York.

19. A. E. Siegel, NATO AGARDograph 91, North Atlantic Treaty Organization Brussels, 1965.

ORNL/TM-11561
Dist. Category UC-420

INTERNAL DISTRIBUTION

1. C. C. Baker
2. L. A. Berry
3. B. A. Carreras
4–8. S. K. Combs
9. R. A. Dory
10. J. L. Dunlap
11. P. W. Fisher
12. C. A. Foster
13. W. Fulkerson
14–18. M. J. Gouge
19. H. H. Haselton
20. J. T. Hogan
21. W. A. Houlberg
22. M. S. Lubell
23–27. S. L. Milora
28. M. J. Saltmarsh
29. T. E. Shannon
30. Director, Fusion Energy Division
31. Laboratory Records, ORNL-RC
32–33. Laboratory Records Department
34–35. Central Research Library
36. Document Reference Section
37. Fusion Energy Division Library
38–39. Engineering Technology/Fusion Energy Division Publications Office
40. ORNL Patent Office

EXTERNAL DISTRIBUTION

41–42. R. W. Kincaid, North Carolina State University, Raleigh, NC 27607
43. Office of the Assistant Manager for Energy Research and Development, U.S. Department of Energy, Oak Ridge Operations Office, P.O. Box E, Oak Ridge, TN 37831
44. J. D. Callen, Department of Nuclear Engineering, University of Wisconsin, Madison, WI 53706-1687
45. R. W. Conn, Department of Chemical, Nuclear, and Thermal Engineering, University of California, Los Angeles, CA 90024
46. N. A. Davies, Acting Director, Office of Fusion Energy, Office of Energy Research, ER-50 Germantown, U.S. Department of Energy, Washington, DC 20545
47. S. O. Dean, Germantown, U.S. Department of Energy, Washington, DC 20545 Fusion Power Associates, Inc., 2 Professional Drive, Suite 248, Gaithersburg, MD 20879
48. H. K. Forsen, Bechtel Group, Inc., Research Engineering, P. O. Box 3965, San Francisco, CA 94119
49. J. R. Gilleland, L-644, Lawrence Livermore National Laboratory, P.O. Box 5511, Livermore, CA 94550
50. R. W. Gould, Department of Applied Physics, California Institute of Technology, Pasadena, CA 91125

51. R. A. Gross, Plasma Research Laboratory, Columbia University, New York, NY 10027
52. D. M. Meade, Princeton Plasma Physics Laboratory, P.O. Box 451, Princeton, NJ 08543
53. M. Roberts, International Programs, Office of Fusion Energy, Office of Energy Research, ER-52 Germantown, U.S. Department of Energy, Washington, DC 20545
54. W. M. Stacey, School of Nuclear Engineering and Health Physics, Georgia Institute of Technology, Atlanta, GA 30332
55. D. Steiner, Nuclear Engineering Department, NES Building, Tibbetts Avenue, Rensselaer Polytechnic Institute, Troy, NY 12181
56. R. Varma, Physical Research Laboratory, Navrangpura, Ahmedabad 380009, India
57. Bibliothek, Max-Planck Institut für Plasmaphysik, Boltzmannstrasse 2, D-8046 Garching, Federal Republic of Germany
58. Bibliothek, Institut für Plasmaphysik, KFA Jülich GmbH, Postfach 1913, D-5170 Jülich, Federal Republic of Germany
59. Bibliothek, KfK Karlsruhe GmbH, Postfach 3640, D-7500 Karlsruhe 1, Federal Republic of Germany
60. Bibliotheque, Centre de Recherches en Physique des Plasmas, Ecole Polytechnique Fédérale de Lausanne, 21 Avenue des Bains, CH-1007 Lausanne, Switzerland
61. R. Aymar, CEN/Cadarache, Departement de Recherches sur la Fusion Contrôlée, F-13108 Saint-Paul-lez-Durance Cedex, France
62. Bibliothèque, CEN/Cadarache, F-13108 Saint-Paul-lez-Durance Cedex, France
63. Library, AEA Fusion, Culham Laboratory, Abingdon, Oxfordshire, OX14 3DB, England
64. Library, JET Joint Undertaking, Abingdon, Oxfordshire OX14 3EA, England
65. Library, FOM-Instituut voor Plasmafysica, Rijnhuizen, Edisonbaan 14, 3439 MN Nieuwegein, The Netherlands
66. Library, National Institute for Fusion Science, Chikusa-ku, Nagoya 464-01, Japan
67. Library, International Centre for Theoretical Physics, P.O. Box 586, I-34100 Trieste, Italy
68. Library, Centro Richerche Energia Frascati, C.P. 65, I-00044 Frascati (Roma), Italy
69. Library, Plasma Physics Laboratory, Kyoto University, Gokasho, Uji, Kyoto 611, Japan
70. Library, Japan Atomic Energy Research Institute, Naka Fusion Research Establishment, 801-1 Mukoyama, Naka-machi, Naka-gun, Ibaraki-ken, Japan

71. Plasma Research Laboratory, Australian National University, P.O. Box 4, Canberra, A.C.T. 2601, Australia
72. Library of Physics Department, University of Ioannina, Ioannina, Greece
73. C. De Palo, Library, Associazione EURATOM-ENEA sulla Fusione, CP 65, I-00044 Frascati (Roma), Italy
74. B. C. Gregory, Centre Canadien de Fusion Magnétique, 1804 Montée Ste-Julie, Varennes, Québec J3X 1S1, Canada
75. T. V. George, Plasma Technologies Branch, Division of Development and Technology, Office of Fusion Energy, Office of Energy Research, ER-531 Germantown, U.S. Department of Energy, Washington, DC 20545
76. W. A. Marton, Plasma Technologies Branch, Division of Development and Technology, Office of Fusion Energy, Office of Energy Research, ER-531 Germantown, U.S. Department of Energy, Washington, DC 20545
77. E. Oktay, Division of Confinement Systems, Office of Fusion Energy, Office of Energy Research, ER-55 Germantown, U.S. Department of Energy, Washington, DC 20545
78. H. S. Staten, Plasma Technologies Branch, Division of Development and Technology, Office of Fusion Energy, Office of Energy Research, ER-531 Germantown, U.S. Department of Energy, Washington, DC 20545
79. S. A. Anderson, Risø National Laboratory, P.O. Box 49, DK-4000 Roskilde, Denmark
80. P. Michelsen, Risø National Laboratory, P.O. Box 49, DK-4000 Roskilde, Denmark
81. D. K. Owens, Princeton Plasma Physics Laboratory, P.O. Box 451, Princeton, NJ 08544
82. G. L. Schmidt, Princeton Plasma Physics Laboratory, P.O. Box 451, Princeton, NJ 08544
83. S. Hibbs, Lawrence Livermore National Laboratory, P.O. Box 5511, Livermore, CA 94550
84. P. Kupschus, JET Joint Undertaking, Abingdon, Oxon OX14 3EA, United Kingdom
85. M. Greenwald, Massachusetts Institute of Technology, 77 Massachusetts Avenue, Cambridge, MA 02139
86. L. Lengyel, Max-Planck-Institut für Plasmaphysik, D-8046 Garching, Federal Republic of Germany
87. A. Reggiori, Politecnico di Milano, P. Leonardo da Vinci, I-20133 Milano, Italy
88. F. Scaramuzzi, ENEA-TIB, I-00044 Frascati (Roma), Italy
89. S. Sudo, Plasma Physics Laboratory, Kyoto University, Gokasho, Uji, Kyoto 611, Japan

90–129. Given distribution as shown in OSTI-4500, Magnetic Fusion Energy (Category Distribution UC-420)